Journal of Materials Chemistry C

Accepted Manuscript

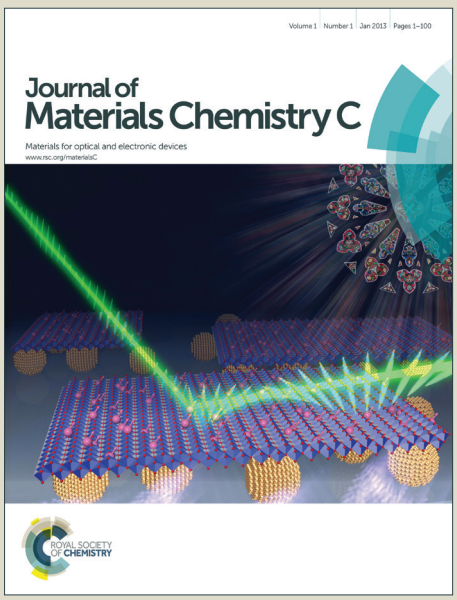

ROYAL SOCIETY OF CHEMISTRY

www.rsc.org/materialsC

Journal Name

RSCPublishing

ARTICLE

A Promising New Nonlinear Optical Crystal with High Laser Damage Threshold for Application in the IR Region: Synthesis, Crystal Structure and Properties of the Noncentrosymmetric $CsHgBr_3$

kCite this: DOI: 10.1039/x0xx00000x

Received 00th January 2012,
Accepted 00th January 2012

DOI: 10.1039/x0xx00000x

www.rsc.org/

Songwei Lv,[a] Qi Wu,[a] Xianggao Meng,[b] Lei Kang,[c] Cheng Zhong,[a] Zheshuai Lin,[c] Zhanggui Hu,[c] Xingguo Chen,[a] Jingui Qin*[a]

Searching for new IR nonlinear optical (NLO) crystals with high laser damage threshold (LDT) has become one of the great challenges in this field. This paper reports the synthesis, single crystal structure and properties of the noncentrosymmetric $CsHgBr_3$, which is a new crystalline phase and shows a high LDT of about 226 MW/cm^2, together with good comprehensive performance. Its crystal can be obtained by reaction of CsBr and $HgCl_2$ in acetone. It crystallizes in the trigonal space group $P3_2$ (No.145). Its powders show a phase-matchable second harmonic generation as strong as that of KH_2PO_4 (KDP). It also displays excellent transparency in the range of 0.42−31 μm and is thermally stable up to 250 °C. All these behaviors make it a promising new NLO crystal in mid-IR region.

1. Introduction

Second-order nonlinear optical (NLO) materials have attracted much attention owing to their uses in laser frequency conversion, optical parameter oscillators, and signal communication.[1, 2] According to the application wavelength ranges, second-order NLO crystal materials can be divided into three main groups, namely ultraviolet NLO crystals, visible NLO crystals, and infrared NLO crystals. In the past decades, several important NLO crystal materials used in the UV and visible regions have been developed, including β-BaB_2O_4 (BBO),[3] LiB_3O_5 (LBO),[4] KH_2PO_4 (KDP),[5] $KTiOPO_4$ (KTP),[6] $LiNbO_3$ (LN).[7] However, excellent NLO crystals for the IR region are much less mature,[8] many current IR NLO crystals such as $AgGaS_2$,[9,10] $AgGaSe_2$,[11] and $ZnGeP_2$,[12] are less suitable for application mainly due to their low laser damage threshold (LDT) and difficulty of crystal growth. In particular, low LDT has become the main obstacle for high-power IR coherent light generation. So the search for new IR NLO crystals with high LDT has become one of the great challenges in this field.

In order to approach this target, the feasibility of halides as such new materials has been investigated in our group[13-18] due to their large energy band gaps that are closely related to high LDT. Some new potential IR NLO materials such as $CsGeCl_3$,[13] $CsCdBr_3$,[14] $HgBr_2$,[15] $Cs_2Hg_3I_8$,[16] $NaSb_3F_{10}$,[17] $Cs_2HgCl_2I_2$[18] have been discovered as potential candidates in this regard. Among these compounds, $Cs_2Hg_3I_8$ has shown very large SHG effect (similar to KTP). However its energy band gap was small (2.56 eV)[16] due to Hg-I bond. To improve the band gap, we had designed and synthesized $Cs_2HgCl_2I_2$, a new NLO crystal with larger band gap (3.15 eV) and much higher LDT (83 MW/cm^2)[18] due to partial replacement of I^- anion. Guided by the idea that the replacement of I^- anions by Br^- or Cl^- anions would further improve LDT, we had tried to synthesize $Cs_aHg_bCl_cBr_{(a+2b-c)}$ in this work. After mixing the solution of CsBr and $HgCl_2$ in acetone, some pale yellow bulk crystals were attained. X-ray single crystal analysis revealed that it is not $Cs_aHg_bCl_cBr_{(a+2b-c)}$ but $CsHgBr_3$. Contrary to the reported $CsHgBr_3$ that was centrosymmetric (space group $Pm\bar{3}$ m and C2/c)[19, 20] and showed no SHG effect, our product shows powder SHG signals as strong as KDP. The single crystal structure analysis confirms that what we obtained is a noncentrosymmetric crystal of $CsHgBr_3$, which has never been reported before. Moreover, this compound possesses very high LDT (226 MW/cm^2), which is seven times as high as that of $AgGaS_2$, a commercialized IR NLO crystal,[21] and wider IR transparent region (0.42−31 μm). All these properties indicate that the new phase of $CsHgBr_3$ is a candidate for NLO materials in the IR region. This paper will report its synthesis, crystal structure and properties.

[a]Department of Chemistry, Wuhan University, Wuhan, 430072. China. E-mail: jgqin@whu.edu.cn
[b]College of Chemistry, Central China Normal University, Wuhan, 430079, China
[c]Beijing Center for Crystal R & D, Technical Institute of Physics and Chemistry, Chinese Academy of Sciences, Beijing 100190, China

2. Experimental Section

2.1 Reagents.

All starting materials were analytical grade from commercial sources. $HgCl_2$, CsBr, and acetone were purchased from Sinopharm and used without further treatment.

2.2 Synthesis of Noncentrosymmetric $CsHgBr_3$.

This compound can be synthesized by conventional solution reaction. Stoichiometric amounts of CsBr (0.852 g, 4 mmol) and $HgCl_2$ (0.544 g, 2 mmol) were carefully dissolved in 40 ml of acetone. The mixture was stirred at 45 °C for 24 h. The colourless reaction mixture was filtered and the filtrate was slowly cooled and evaporated at room temperature. After 45 days, the pale yellow bulk crystals of $CsHgBr_3$ (0.701 g, with 61.1 % yield) were obtained (a photograph of a crystal is shown in Figure S2 in the supporting Information).

2.3 Single Crystal Structure Determinations.

A single crystal of $CsHgBr_3$ with dimensions of ca. 0.10 × 0.05 × 0.02 mm^3 was selected and used for the single-crystal diffraction experiment. Data sets were collected using a Bruker SMART APEX diffractometer equipped with a CCD detector (graphite-monochromated Mo Kα radiation, λ =0.71073 Å) at 296(2) K. Data set reduction and integration were performed using the software package SAINTPLUS.[22] The crystal structure was solved by direct methods and refined using the SHELXTL 97 software package.[23] Single crystal data collection, cell parameters, and basic information for $CsHgBr_3$ are summarized in Table 1.

Table 1. Crystallographic data of $CsHgBr_3$ in this work

Empirical formula	$CsHgBr_3$
Formula weight	573.23
T/K	296(2)
Wavelength/ Å	0.71073
Crystal color	Pale Yellow
Space group	$P3_2$ (No. 145)
a/ Å	8.0479(19)
b/ Å	8.0479(19)
c/ Å	9.904(3)
α / °	90.00
β / °	90.00
γ / °	120.00
Volume/ $Å^3$	555.5(3)
Z	3
d_{cal}/ g cm^{-3}	5.141
F(000)	720
Crystal size/ mm	0.10 × 0.05× 0.02
Reflections collected	1260
Independent reflections	556
R_1, wR_1 [I > 2σ(I)]	0.0687/0.1582
R_2, wR_2 (all data)	0.1143/0.1932
Min/max Δρ/ e $Å^{-3}$	-2.058/2.513
$w=1/[\sigma^2(Fo^2)+(0.1907P)^2+0.0000P]$	
Where $P=(Fo^2+2Fc^2)/3$	

2.4 Powder X-ray Diffraction.

X-ray powder diffraction (XRD) patterns of polycrystalline material were collected using a Bruker D8 Advance diffractometer with Cu Kα1 radiation (λ=1.54186 Å) in the range of 10 -70° (2θ) at a scanning rate of 1 °/min. The powder XRD patterns for $CsHgBr_3$ obtained from solution reaction showed good agreement with the calculated XRD patterns based on the single-crystal structure analysis results (see Figure S3 in the Supporting Information).

2.5 Infrared Spectrum, Raman Spectrum, and UV-Vis Diffuse Reflectance Spectrum.

The optical transmission spectrum in the mid-IR region was run on a NICOLET 5700 Fourier-transformed infrared (FTIR) spectrophotometer in the 4000-700 cm^{-1} region (2.5-14 μm) using the attenuated total reflection (ATR) technique with a germanium crystal. The Raman scattering spectrum in the 800-100 cm^{-1} region (12.5-100 μm) was carried out using a Renishaw RM 1000 laser confocal Raman microspectrometer at room temperature. The 514.5 nm line of an Ar-ion laser was used for excitation. The ATR-FTIR spectrum and the Raman spectrum were performed on $CsHgBr_3$ crystal. The UV-vis absorption spectrum was performed on a Varian Cary 5000 UV-vis-NIR spectrophotometer in the region 200-800 nm. A $BaSO_4$ plate was used as the standard (100% reflectance), on which the finely ground samples from the crystals were coated. The absorption spectrum was calculated from the reflectance spectra using the Kubelka-Munk function: $\alpha/S= (1-R)^2/(2R)$,[24] where α is the absorption coefficient, S is the scattering coefficient, and R is the reflectance.

2.6 NLO Property and LDT Measurements.

The NLO efficiencies of the samples were investigated using a Kurtz-Perry power technique.[25] A pulsed Q-switched Nd:YAG laser was utilized to generate fundamental 1064 nm light with a pulse width of 10 ns. Microcrystalline KDP was served as the standard. Laser-induced damage test was performed[15, 17] on small crystalline samples without any pretreatment, with 10 Hz focused laser pulses emitted by the laser source (1064 nm, 5 ns). The energy of each pulse was measured to be about 200 mJ. An optical concave lens was used to adjust the diameter of the laser beam to obtain different intensity. The samples endured gradually enhanced radiation until their appearance changed under a magnifier after the irradiation.

2.7 Thermogravimetric Analysis.

The thermogravimetric analysis (TGA) was carried out on SETSYS-16 simultaneous analyzer instrument. The crystal sample was added into an Al_2O_3 crucible and heated from room temperature to 800 °C at a heating rate of 10 K/min under flowing nitrogen gas.

2.8 First Principles Calculations.

The first-principles electronic structure calculations on $CsHgBr_3$ are performed by the plane-wave pseudopotential method[26] implemented in the CASTEP program[27] based on density functional theory (DFT).[28] The Perdew-Burke-Ernzerhof (PBE) functionals of generalized gradient approximation (GGA)[29] is adopted. The ion-electron interactions are modeled by the optimized norm-conserving pseudopotentials[30] of the Kleinman-Bylander form[31] for all constituent elements, and Cs $5s^25p^66s^1$, Hg $5d^{10}6s^2$, and Br $4s^24p^5$ electrons are treated as the valence electrons, respectively. The kinetic energy cutoff of 900 eV and Monkhorst-Pack k-point meshes[32] spanning less than 0.04/$Å^3$ in the Brillouin zone are chosen to ensure the sufficient accuracy for present purpose.

3. RESULTS AND DISCUSSION

3.1 Synthesis.

Originally what we planned to synthesize was a mixed-halide compound, $Cs_aHg_bCl_cBr_{(a+2b-c)}$. For that purpose, Stoichiometric amounts of CsBr (0.852 g, 4 mmol) and $HgCl_2$ (0.544 g, 2 mmol) were carefully dissolved in 40 ml of acetone. The mixture was stirred at 40 °C for 8h. The colourless solution was filtered and slowly cooled and evaporated at room temperature. The pale yellow bulk crystals were obtained. However, the Energy Dispersive X-Ray Spectroscopy (EDX) and X-ray single crystal analysis indicate that the crystal is $CsHgBr_3$ with a noncentrosymmetric crystal structure and it was SHG active. Actually, we had such kind of experience before. For instance, in our previous work, we obtained $CsCdBr_3$ instead of $Cs_aCd_bBr_cI_{(a+2b-c)}$ through mixing CdI_2's acetone solution and CsBr's acetone solution.[14] In another case, we obtained $Cs_2Hg_3I_8$instead of $Cs_aHg_bBr_cI_{(a+2b-c)}$ from the reaction of HgI_2 and CsBr in acetone.[16] This unexpected result may be explained by the Hard-Soft-Acid-Base (HSAB) theory. According to HSAB theory, Hg^{2+} is a softer acid compared to Cd^{2+}, and I^- is a softer base than Br^-, and even much more softer than Cl^-. As a result, in the work of this paper, the binding capacity of the soft acid Hg^{2+} is greater with the softer bases Br^- than the hard base Cl^-. In the other words, when CsBr meets with $HgCl_2$ in solution, Cl^- tends to be replaced gradually by Br^-, and in the end, the noncentrosymmetric $CsHgBr_3$ was obtained. On the other hand, in the literature,[19, 20] $CsHgBr_3$ was synthesized before by reaction of CsBr and $HgBr_2$ in acetone. But they belong to centrosymmetric space groups, either Pm2$_1$m [19] or C2/c[20]. It seems that the reason for this reaction to produce the centrosymmetric $CsHgBr_3$ might be that there was no Cl^- anion in the reaction system of CsBr with $HgBr_2$, and there was no need for Br^- anion to replace the Cl^- anion so as to produce $CsHgBr_3$. We have tried to repeat this reaction following the literate description[20]. What we obtained by this method was colorless and exhibited no SHG effect. So we confirm that what we have prepared from the reaction of CsBr and $HgCl_2$ in acetone is a new phase of $CsHgBr_3$ with a noncentrosymmetric crystal structure, which has never been reported before.

3.2 Crystal Structure.

Single-crystal X-ray diffraction data for our $CsHgBr_3$ is presented in Table 1. It belongs to trigonal structure with a noncentrosymmetric space group, $P3_2$. Its cell parameters are: a = 8.0479 (19) Å, b = 8.0479 (19) Å, c =9.904(3) Å, α=90 °, β=90 °, γ=120 °, Z=3, and V=555.5(3) Å^3.

Figure 1 shows the ball-and-stick diagrams of $CsHgBr_3$. In the structure, one mercury atom and six bromide atoms form an octahedron (Figure 1b). The octahedral are not isolated, due to the existence of bromine atom bridged linkage between two Hg atoms giving rise to the three dimensional structure. The structure of the compound is simple and similar to $CsHgCl_3$.[33] Each $HgBr_6$ octahedron is distorted, as three long Hg–Br bond lengths are 3.021, 3.183 and 3.225 Å, respesctively, while the other three short Hg–Br bond lengths are 2.494, 2.501 and 2.689 Å, respesctively. It is worth comparing the structure difference between our noncentrosymmetric crystal and the reported centrosymmetric one.[20] They are two polymorphs of $CsHgBr_3$ and have similar distorted octahedron anionic unit [$HgBr_6$]. But the packing styles of the octahedra are different. In the reported centrosymmetric $CsHgBr_3$ with the monoclinic space group C2/c[20], the distorted $HgBr_6$ octahedra are connected in a centrosymmetric style. On the other hand, in our noncentrosymmetric crystal of $CsHgBr_3$, the distortion directions of all the octahedral are almost parallel as indicated in Figure 1a, which is beneficial to an additive superimposition of the microscopic second-order susceptibilities of each octohedron, leading to the exhibition of a strong macroscopic NLO effect in crystal.[34]

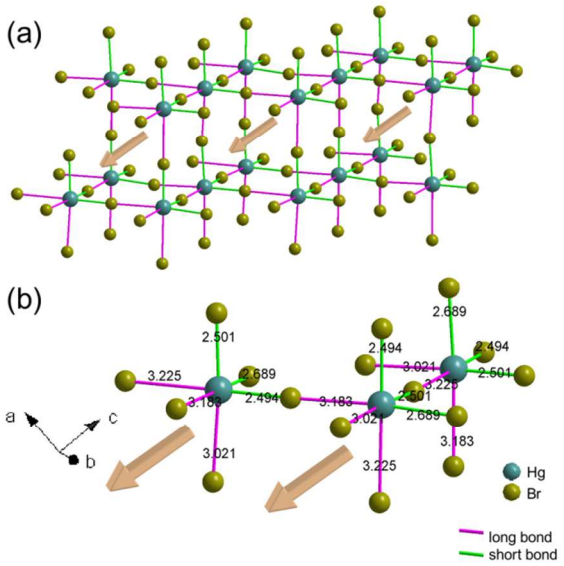

Figure 1. (a) Ball-and-stick diagram of $CsHgBr_3$ crystal (Cs atoms are omitted for clarity). The shorter Hg-Br bonds are always located in the upper right corner in each $HgBr_6$ octahedron, giving rise to a net dipole moment antiparallel to the c axis (indicated by the arrow). (b) Ball-and-stick diagram of $HgBr_6$ octahedron in a unit cell. Each octahedron is distorted, giving rise to a net dipole moment antiparallel to the c direction.

3.3 Optical Properties.

The ATR-FTIR spectrum and Raman spectrum of $CsHgBr_3$ crystalline samples are shown in Figures 2 and 3, respectively. The ATR-FTIR spectrum shows no absorption in the middle IR region from 4000 to 700 cm^{-1} (2.5–14 μm). The Raman spectrum was collected in the region from 800 to 100 cm^{-1} (12.5–100 μm). There is no absorption in the region from 800 to 318 cm^{-1} (12.5–31 μm). These facts indicate that the transparency edge of $CsHgBr_3$ reaches 31 μm at far-IR side. The UV-vis diffuse reflectance spectrum for $CsHgBr_3$ is shown in Figure 4. The compound is pale yellow, the spectrum shows that the absorption edge near the UV side is at about 414 nm, indicating that the optical band gap of the compound is approximately 3.0 eV, which is higher than the commercial IR NLO crystals such as $AgGaS_2$ (2.76 eV). Based on these data, the transparent range of $CsHgBr_3$ powders is 0.42-31 μm.

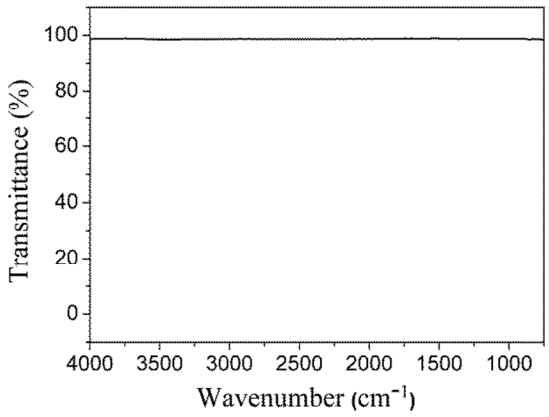

Figure 2. ATR-FTIR spectrum of $CsHgBr_3$ crystal.

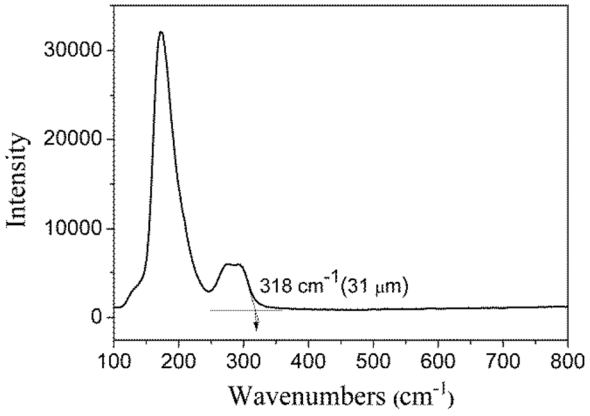

Figure 3. Raman spectrum of $CsHgBr_3$ crystal.

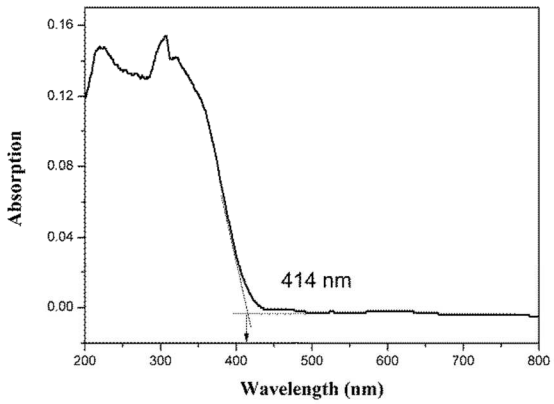

Figure 4. UV-vis spectrum of $CsHgBr_3$ microcrystalline sample.

3.4 NLO Property and LDT Measurements.

Powder SHG measurements using 1064 nm laser radiation revealed that $CsHgBr_3$ showed power SHG efficiencies as strong as KDP. Study result of the SHG intensity as a function of particle size (from 40 to 300 μm) is shown in Figure 5. The intensity of the SHG signals at first increases gradually with the increase of the sample size and then reaches a saturasion when the sample size increases further. It is a typical curve of the phase-matchable materials.[25]

A preliminary examination of the laser-induced damage threshold has been carried out on crystalline sample with a Q-switched laser source.[15, 17] The samples showed a damage threshold of about 226 MW/cm^2 (1064 nm, 5 ns), which is much higher than that for $AgGaS_2$ of 30 MW/cm^2.[21]

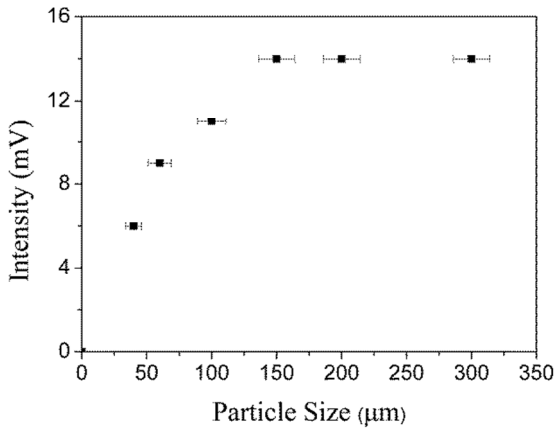

Figure 5. Dependence of SHG intensity on the particle size.

3.5 Thermogravimetric Analysis.

The thermal behavior of $CsHgBr_3$ was investigated using thermogravimetric analysis (TGA). The compound is thermally stable up to 250 °C. From 250 to 520 °C, the compound loses weight until about 35% remains. This implies that the residue is mainly CsBr (whose weight portion in $CsHgBr_3$ is 37.1%). The pale yellow crystal is not hygroscopic.

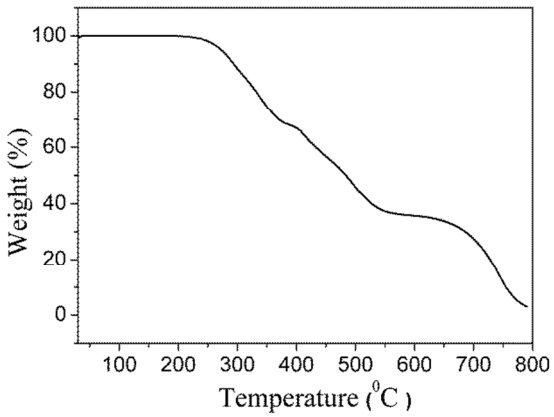

Figure 6. Thermogravimetric analysis curve for $CsHgBr_3$ crystal.

3.6 First Principles Electronic Structure Study.

The electronic density of states (DOS) and partial DOS (PDOS) of $CsHgBr_3$ is displayed in Figure 7. It is clear that the energy region below –5 eV is mainly composed of the isolated inner orbitals of Cs (5s) (5p), Hg (5d), and Br (5s), which are strongly localized deep in the valence band (VB) and have a negligible influence on the IR optical properties. The top of the VB and the bottom of conduction band (CB) are mainly occupied by the orbitals of Hg (6s) and Br (5p). It should be emphasized that the states on both sides of the energy band gap are mainly composed of the orbitals from the $[HgBr_6]^{4-}$ anionic

units, while nearly nothing contributed from the Cs^+. Since the optical response of a crystal in the visible-IR region mainly originates from the electronic transitions between the VB and CB states close to the band gap,[35] the $[HgBr_6]^{4-}$ anionic units determine the optical properties of $CsHgBr_3$, in accordance with the anionic group theory proposed by Chen[36] for the ultraviolet NLO crystals.

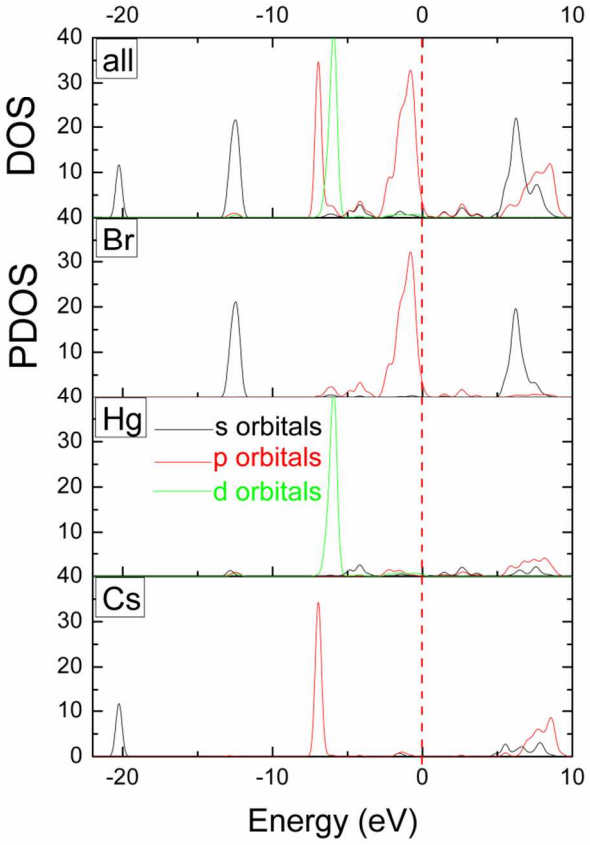

Figure 7. The calculated DOS and PDOS for $CsHgBr_3$.

4 Conclusion

In summary, the new phase of $CsHgBr_3$ with noncentrosymmetric crystalline structure has been obtained by reaction of CsBr and $HgCl_2$ in acetone. The intensity of second harmonic generation effect is comparable with that of KDP and the effect is phase-matchable. The compound is transparent in the range of 0.42-31 μm. A preliminary measurement indicates that its laser-induced damage threshold is quite high (about 2.87 MW/cm^2). The material is thermally stable up to 250 °C and its single crystals can be grown by slow solvent evaporation technique. Owing to these properties, $CsHgBr_3$ appears to be a promising new NLO crystal applicable in the infrared region.

Acknowledgements

This work was supported by the National Science Foundation of China (Grant Nos. 91022036 and 11174297) and the National Key Foundation (973) Program of China (Grant No. 2010CB630701). We thank Mr. Xiaomao Li and Mr. Zhenhua Cao of Technical Institute of Physics and Chemistry, Chinese Academy of Sciences, China for their help with LDT and SHG measurement.

Notes and references

(1) D. M. Burland, R. D. Miller, C. A. Walsh, *Chem. Rev*. 1994, **94** (1), 31-75.
(2) B. H. T. Chai, Optical Crystals. In CRC Handbook of Laser Science and Technology, Supplement 2: Optical Materials; Weber, M. J., Ed.; CRC Press: Boca Raton, FL, 1995; pp 3-65.
(3) C. Chen, B. A. Jiang, G. You, Sci. Sin., Ser. B 1985, 28 (3), 235-243.
(4) C. Chen, Y. Wu, A. Jiang, G. You, R. Li, S. Lin, *J. Opt. Soc. Am. B* 1989, **6** (4), 616-621.
(5) W. L. Smith, *Appl. Opt*. 1977, **16** (7), 798.
(6) K. Kato, *IEEE J. Quantum Electron*. 1991, **27**, 1137-1140.
(7) G. D. Boyd, R. C. Miller, K. Nassau, W. L. Bond, A. Savage, *Appl. Phys. Lett*. 1964, **5** (11), 234-236.
(8) Y. M. Xie, R. M. Yu, X. Y. Wu, S. C. Chen, C. Lu, *Z CrystEngComm*. 2010, **12**, 3490-3492.
(9) D. S. Chemla, P. J. Kupecek, D. S. Robertson, R. C. Smith, *Opt. Commun*. 1971, **3** (1), 29-31.
(10) A. O. Okorogu, S. B. Mirov, W. Lee, D. I. Crouthamel, N. Jenkins, A. Y. Dergachev, K. L. Vodopyanov, V. V. Badikov, *Opt. Commun*. 1998, **155**, 307-312.
(11) G. D. Boyd, H. Kasper, J. H. McFee, F. G. Storz, *IEEE J. Quant. Electron*. 1972, **QE-8** (12), 900-908.
(12) G. D. Boyd, E. Buehler, F. G. Storz, *Appl. Phys. Lett*. 1971, **18** (7), 301-304.
(13) J. Zhang, N. Su, C. Yang, J. G. Qin, N. Ye, B. C. Wu, C. T. Chen, *Proc. SPIE*, 1998, 3556, 1.
(14) P. Ren, J. G. Qin, C. T. Chen, *Inorg. Chem*. 2003, **42**, 8-10.
(15) T. Liu, J. G. Qin, G. Zhang, T. X. Zhu, F. Niu, Y. C. Wu, C. T. Chen, *Appl. Phys. Lett*. 2008, **93**, No. 091102.
(16) G. Zhang, J. G. Qin, T. Liu, P. Fu, Y. C. Wu, C. T. Chen, *Cryst. Growth. Des*. 2008, **8**, 2946-2949.
(17) G. Zhang, J. G. Qin, T. Liu, Y. J. Li, Y. C. Wu, C. T. Chen, *Appl. Phys. Lett*. 2009, **95**, No. 261104.
(18) G. Zhang, Y. J. Li, K. Jiang, H. Y. Zeng, T. Liu, X. G. Chen, J. G. Qin, Z. S. Lin, Y. C. Wu, C. T. Chen, *J. Am. Chem. Soc*. 2012, **134**, 14818-14822.
(19) G. Natta, L. Passerini, *Gazzetta Chimica Italiana.* 1928, **58**, 472-484.
(20) S. Walha, J. M. Savariault, J. Jaud, A. B. Salah, *Phys. Chem. News*. 2002, **8**, 69-78.
(21) S. Chandra, T. H. Allik, G. Catella, J. A. Hutchinson, Advanced Solid-State Lasers; Bosenberg, W. R.; Fejer, M. M., Eds.; OSA Trends in Optics and Photonics Series, Vol. 19; OSA: Washington, DC, 1998, pp 282-284.
(22) G. M. Sheldrick, SHELXTL, version 6.14, Bruker Analytical X-ray Instruments, Inc, Madison, WI, USA, 2003.
(23) G. M. Sheldrick, *Acta Crystallogr*. 2008, **A64**, 112-122.
(24) W. M. Wendlandt, H. G. Hecht, Reflectance Spectroscopy; Interscience: New York, 1966, pp 62-65.
(25) S. K. Kurtz, T. T. Perry, *J. Appl. Phys.* 1968, **39**, 3798-3813
(26) M. C. Payne, M. P. Teter, D. C. Allan, T. A. Arias, J. D. Joannopoulos, *Rev. Mod. Phys*. 1992, **64** (4), 1045-1097.
(27) S. J. Clark, M. D. Segall, C. J. Pickard, P. J. Hasnip, M. J. Probert, K. Refson, M. C. Payne, *Zeitschrift. Fur. Kristallographie*. 2005, **220** (5-6), 567-570.
(28) W. Kohm, L. J. Sham, *Phys. Rev*. 1965, **140** (4A), 1133-1138.
(29) J. P. Perdew, Y. Wang, *Phys. Rev. B* 1992, **45** (23), 13244-13249.
(30) J. S. Lin, A. Qteish, M. C. Payne, V. Heine, *Phys. Rev. B* 1993, **47** (8), 4174-4180.
(31) L. Kleinman, D. M. Bylander, *Phys. Rev. Lett*. 1982, **48** (20), 1425-1428.
(32) H. J. Monkhorst, J. D. Pack, *Phys. Rev. B* 1976, **13** (12), 5188-5192.
(33) O. Albarski, H. Hillebrecht, H. W. Rotter, G. Thiele, *Z. Anorg. Allg. Chem*. 2000, **626**, 1296-1304.
(34) P. S. Halasyamani, K. R. Poeppelmeier, *Chem. Mater*. 1998, **10**, 2753-2769.
(35) M. H. Lee, C. H. Yang, J. H. Jan, *Phys. Rev. B*. 2004, **70** (23), 235110.

(36) C. T. Chen, T. Sasaki, R. K. Li, Y. C. Wu, Z. S. Lin, Y. Mori, Z. G. Hu, J. Y. Wang, S. Uda, M. Yoshimura, Y. Kaneda, Wiley-VCH press: Germany, 2012.

A Promising New Nonlinear Optical Crystal with high laser damage threshold for application in the IR Region: Synthesis, Crystal Structure and Properties of the Noncentrosymmetric $CsHgBr_3$

Songwei Lv,[†] Qi Wu,[†] Xianggao Meng,[‡] Lei Kang,[ξ] Cheng Zhong,[†] Zheshuai Lin,[ξ] Zhanggui Hu,[ξ] Xingguo Chen,[†] Jingui Qin[†]*

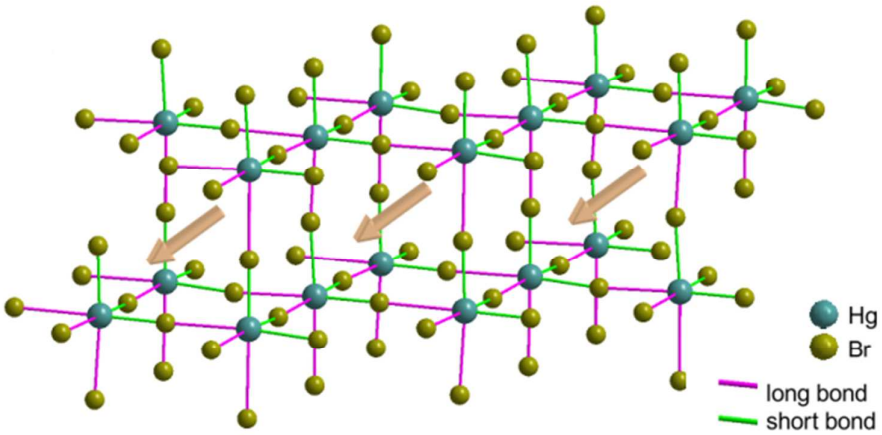

A new phase of $CsHgBr_3$ with noncentrosymmetric crystalline structure is synthesised and shows high laser damage threshold and nonlinear optical property.